EC
Journals.ASM.org

Developmental Coordination of Gamete Differentiation with Programmed Cell Death in Sporulating Yeast

Michael D. Eastwood, Marc D. Meneghini

Department of Molecular Genetics, University of Toronto, Toronto, Ontario, Canada

The gametogenesis program of the budding yeast *Saccharomyces cerevisiae*, also known as sporulation, employs unusual internal meiotic divisions, after which all four meiotic products differentiate within the parental cell. We showed previously that sporulation is typically accompanied by the destruction of discarded immature meiotic products through their exposure to proteases released from the mother cell vacuole, which undergoes an apparent programmed rupture. Here we demonstrate that vacuolar rupture contributes to *de facto* programmed cell death (PCD) of the meiotic mother cell itself. Meiotic mother cell PCD is accompanied by an accumulation of depolarized mitochondria, organelle swelling, altered plasma membrane characteristics, and cytoplasmic clearance. To ensure that the gametes survive the destructive consequences of developing within a cell that is executing PCD, we hypothesized that PCD is restrained from occurring until spores have attained a threshold degree of differentiation. Consistent with this hypothesis, gene deletions that perturb all but the most terminal postmeiotic spore developmental stages are associated with altered PCD. In these mutants, meiotic mother cells exhibit a delay in vacuolar rupture and then appear to undergo an alternative form of PCD associated with catastrophic consequences for the underdeveloped spores. Our findings reveal yeast sporulation as a context of bona fide PCD that is developmentally coordinated with gamete differentiation.

Sporulation represents the most dramatic developmental occurrence during the life cycle of *Saccharomyces cerevisiae* (here referred to as yeast). Diploid yeast cells execute sporulation in response to conditions of nutritional stress, when environmental nitrogen and fermentable sugars are lacking. The presence of at least some nonfermentable carbon is crucial for the initiation of meiosis. Upon encountering these starvation conditions, cells execute meiosis that is coupled with the differentiation of meiotic products into highly stress-resistant and dormant gametes called spores (1). Sporulation thus serves as both the gametogenesis phase of the yeast sexual cycle and a stress response during periods of starvation.

Yeast meiosis occurs with no intervening karyokinesis, resulting in the sequestration of haploid complements of chromosomes to four lobes of the parental nucleus. *De novo*-formed prospore double membranes subsequently envelop each lobe, pinching off to produce new daughter nuclei as they complete cellularization. Within the lumen of these double membranes occurs the ordered assembly of a multilayered cell wall called the spore coat, which confers stress resistance and durability to mature spores (Fig. 1A). The inner prospore membrane then serves as the plasma membrane of the spore. Terminal spore maturation is associated with a tightening of the mother cell remnant, which encapsulates the spores in a structure called the ascus (1). Although electron micrograph studies have shown that at least 70% of the cellular content of the mother cell is not inherited by the newly produced spores (2), the developmental fate of the mother cell *per se* has remained nearly uninvestigated.

Under conditions of limiting carbon availability, only approximately half of the meiotic products are subject to spore development, a phenomenon known as spore number control (3–5). We showed previously that these discarded meiotic products are digested by vacuolar proteases, which gain access to the immature gametes through the apparent programmed rupture of the vacuolar membrane (6). This phenomenon, which we termed programmed nuclear destruction (PND), is accompanied by nucleosome-sized fragmentation of genomic DNA from the discarded nuclei. PND-associated nucleosomal cleavage is dependent on Nuc1, a highly conserved mitochondrial nuclease of the endonuclease G (endoG) family that has been implicated in the death of vegetative yeast cells exposed to oxidative stress and in animal cell apoptosis (6, 7). These findings prompted questions concerning the evolution of programmed cell death (PCD) (8). Although PCD is known to occur in unicellular microbes in response to various stresses, how PCD came about in these organisms, and indeed generally, has remained a quandary. PCD is hypothesized to have evolved by harnessing mechanisms that were initially nonlethal for the cell, and yeast PND was suggested to represent an example of such nonlethal applications of cell death mechanisms (8).

To better understand the relationship of PND and PCD, we shifted our emphasis from the fate of the discarded nuclei to that of the meiotic mother cell itself. As discarded meiotic products subject to PND do not acquire a prospore/plasma membrane and remain within the mother cell cytoplasm (6), we hypothesized that PND is actually the consequence of these nuclei being swept up into a PCD of the mother cell. In this study, we explore this hypothesis by examining the fate of the meiotic mother cell and its organelles following meiotic cell division (prospore membrane

Received 17 April 2015 **Accepted** 17 June 2015

Accepted manuscript posted online 19 June 2015

Citation Eastwood MD, Meneghini MD. 2015. Developmental coordination of gamete differentiation with programmed cell death in sporulating yeast. Eukaryot Cell 14:858–867. doi:10.1128/EC.00068-15.

Address correspondence to Marc D. Meneghini, marc.meneghini@utoronto.ca.

Supplemental material for this article may be found at http://dx.doi.org/10.1128/EC.00068-15.

doi:10.1128/EC.00068-15

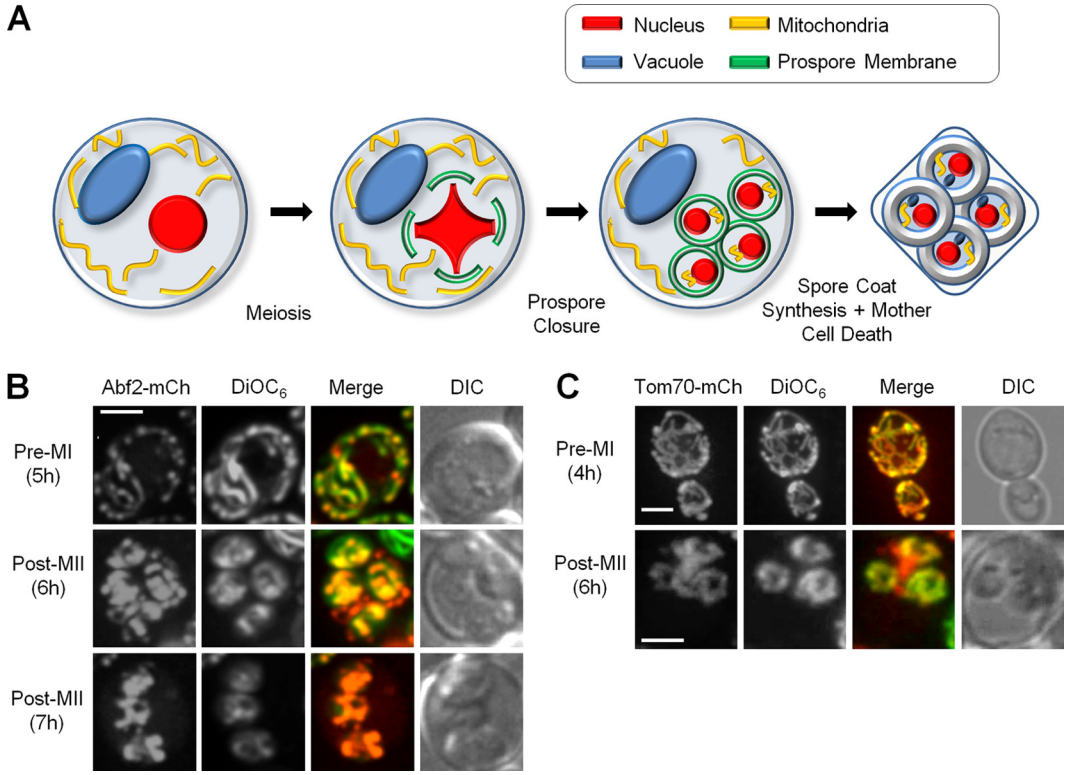

FIG 1 Cells committed to meiosis exhibit mitochondrial depolarization. (A) The meiotic mother cell retains the majority of its contents upon prospore cellularization, including all of its vacuoles and half of its mitochondria. When sporulation is complete, the mother cell is no longer present, having undergone autolysis. Vacuoles are regenerated in mature spores. (B) Comparison of Abf2-mCherry-containing mitochondria and $DiOC_6$-positive mitochondria in premeiotic (5 h postinduction) (top) and early postmeiotic (6 h postinduction) (middle) stages. Mitochondria are no longer detectable 7 h after induction (bottom). (C) Overlap of Tom70-mCherry- and $DiOC_6$-labeled mitochondria at 4 h (top) and 6 h (bottom) postinduction. Bars = 2 μm (all panels). DIC, differential interference contrast.

closure). We find that soon after meiotic cell division is complete, the mother cell initiates dramatic organellar changes characteristic of cells executing PCD. Examination of mother cell death in various spore morphogenesis mutants revealed that cells compromised for spore formation execute delayed and morphologically distinct PCD. Our observations suggest that mother cell death represents bona fide developmental PCD intrinsic to sporulation that shares common regulation with spore morphogenesis. Consistent with conclusions from our previous study (6), the rupture of the vacuole plays a central role in the execution of mother cell PCD. Indeed, the yeast vacuole is analogous to lysosomes found in animal cells, which were originally characterized as "suicide bags" (9) and interface with animal PCD pathways in a diverse array of mechanisms (10). Our findings provide further support for the view of this phenomenon as an example of PCD mechanisms which may have arisen early in eukaryotic evolution (8).

MATERIALS AND METHODS

Yeast strains. Strains used in this study are described in Table S1 in the supplemental material and are of the SK1 background. Standard *S. cerevisiae* culture and genetic techniques were used for strain construction. All strains were constructed for the purpose of this study, with the exception of MMY718 and MEY238 (6). Tagging of endogenous proteins with mCherry was accomplished by using long-oligonucleotide-based C-terminal tagging. In the case of Pma1-mCherry, we engineered an extended linker region of 18 additional amino acids, a GGS triplet repeated 6 times, to maintain the functionality of Pma1-mCherry. Gene deletions were constructed by replacing the open reading frames (ORFs) of interest with a G418 resistance cassette (KanMX4), using standard methods.

Sporulation protocols. Sporulation was conducted by using liquid medium. Strains were recovered from freezer stocks, added to plates containing 1% yeast extract–2% peptone (YP) and 2% glycerol–3% ethanol, and allowed to grow overnight, and then single colonies were isolated on YP–2% dextrose (YPD) medium. Colonies were inoculated into liquid YPD medium, grown to saturation overnight, diluted into presporulation medium (YP plus 3% potassium acetate [YPA]) at an optical density at 600 nm (OD_{600}) of 0.3, and cultured for 12 to 14 h with vigorous aeration (200 rpm). YPA cultures were harvested at an OD_{600} of 1.5 to 1.8, washed twice in deionized (dI) water, and resuspended in sporulation medium (1% potassium acetate, 0.02% raffinose) at an OD_{600} of 2.0. Colonies from low-carbon sporulations were cultured identically up to sporulation induction, at which point they were suspended in fresh 0.1% potassium acetate for 5 h, pelleted, and resuspended in an equal volume of 0.15% potassium chloride. In experiments utilizing inducible *NDT80* induction, expression of *NDT80* with β-estradiol was induced by diluting a 5 mM β-estradiol stock in 100% ethanol directly into the sporulating culture at a final concentration of 1 μM after 5.5 h of incubation of cells in sporulation medium.

Light microscopy. Live-cell confocal microscopy was used to generate light microscopy data. Cells were mounted directly from liquid sporulation medium onto 2% agarose pads made with sporulation medium. Pads were solidified on standard microscope slides, loaded with ~4.5×10^5 cells suspended in 10 μl, enclosed with a coverslip, and adhered to the slide with valap at the corners. Cells were imaged within 30 min of agarose mounting. All light microscopy data are three-dimensional (3-D) images

reconstructed from z-stacks captured by using a Leica DMI6000 microscope equipped with a WaveFX spinning-disc confocal system with a z-plane spacing of 1 μm, except where single focal planes are presented, as indicated. Images were constructed by using Volocity High Performance 3-D 4-D imaging software.

For mitochondrial $DiOC_6$ imaging, ~1×10^7 cells in 1 ml were resuspended in an equal volume of sporulation medium plus 10 mM HEPES (pH 7.4) immediately prior to staining. $DiOC_6$ (Sigma) was added at 500 ng/ml from a 10-mg/ml stock made in 100% ethanol. Cells were incubated for 20 min at room temperature, washed three times with sporulation medium plus 10 mM HEPES (pH 7.4), and mounted for imaging as described above.

Propidium iodide (PI) was purchased as part of the annexin V fluorescein isothiocyanate (FITC) detection kit (Sigma). One microliter of a propidium iodide stock was added to ~9×10^5 cells suspended in 40 μl of sporulation medium plus 10 mM HEPES (pH 7.4) and incubated for 20 min at room temperature. Cells were then washed three times in sporulation medium plus 10 mM HEPES (pH 7.4) and mounted for imaging as described above.

For osmotic stress experiments, 2 μl of 5 M NaCl was added to ~9×10^5 cells suspended in 23 μl of sporulation medium to a final concentration of 400 mM NaCl, incubated for 10 min at room temperature, and mounted for immediate imaging.

Transmission electron microscopy. Transmission electron microscopy (TEM) samples were preserved by using a Leica HMP100 high-pressure freezing system (11), with minimal modifications. Embedded cells were sectioned into 50-nm-thin sections and imaged with an FEI Tecnai 20 transmission electron microscope and an AMT 16000 digital camera.

Cell viability assays. Following initial suspension in sporulation medium, a defined volume of culture medium was plated such that at least 600 distinct colonies were counted. After 24 h of sporulation, the same volume was plated, and colonies were counted. Survival was assessed as the ratio of the number of CFU/volume after 24 h to the number of CFU/volume at induction.

RESULTS

Meiotic mother cells exhibit mitochondrial dysfunction and vacuole swelling. To address the hypothesis that meiotic mother cells execute PCD, we examined the characteristics of organelles retained in the mother cell to compare them with established PCD-related phenomena. Unless otherwise indicated, all of our studies were performed under standard (high-carbon) sporulation conditions, which disfavor PND and promote survival of all meiotic products (6). Thus, the meiotic mother cell characteristics that we describe occur independent of PND and spore number control and represent core aspects of yeast sporulation. Moreover, when we use the term "meiosis," we are referring specifically to the period during which the segregation of chromosomes during meiosis I (MI) and meiosis II (MII) occurs. PND, spore development, and the to-be-described meiotic mother cell PCD occur following meiosis.

Loss of mitochondrial membrane potential (Δψ) underlies diverse types of PCD (12–14). To begin to investigate the fate of the gametogenic mother cell, we examined the properties of its mitochondrial Δψ. To monitor mitochondrial Δψ during sporulation, we adapted a method previously utilized with replicatively aged yeast cells (15). We visualized total cellular mitochondria using an Abf2-mCherry fusion protein, which localizes to mitochondrial nucleoids. By simultaneously treating these cells with $DiOC_6$ (3,3′-dihexyloxacarbocyanine iodide), a lipophilic dye that stains Δψ-positive mitochondria, we discerned active mitochondria ($DiOC_6$ positive [$DiOC_6^+$]and Abf2-mCherry positive) compared to total mitochondria (Abf2-mCherry positive only). All cells that had not completed meiosis maintained strong overlap between Abf2-mCherry and $DiOC_6$ (Fig. 1B). Consistent with previously reported findings (2), as immature spores formed within the meiotic mother cell, we observed that some mitochondria remained within the mother cell. During this early postmeiotic stage, however, we found that mitochondria that were retained in the mother cell lacked a $DiOC_6$ signal, while those that segregated into the developing spores were $DiOC_6^+$. These cells were stained with $DiOC_6$ immediately prior to meiotic nuclear segregation, suggesting that mother cell mitochondria lost Δψ, while those in the developing spores preserved it (Fig. 1B). The loss of Δψ was detectable very soon after the completion of meiosis: as soon as we were able to distinguish that Abf2-mCherry mitochondria had been segregated to prospores, we observed a loss of $DiOC_6$ staining in those remaining within the mother cell. We found that 96.4% ± 1.5% of postmeiotic cells scored 7 h after sporulation induction clearly exhibited a specific loss of the $DiOC_6$ signal within the mother cell ($n = 3$; $n > 150$). Interestingly, as spore development progressed, mitochondria were no longer detected in the mother cell (Fig. 1B).

We confirmed our above-described findings with similar imaging experiments utilizing the outer mitochondrial membrane marker Tom70-mCherry. As with our Abf2-mCherry experiments, these studies confirmed that mitochondria that were retained in the mother cell lacked Δψ. Moreover, these studies revealed that depolarized mother cell mitochondria appeared to aggregate and potentially swell in early postmeiotic cells (Fig. 1C). In addition to involving a loss of mitochondrial Δψ, necrotic forms of cell death are associated with a general swelling of organelles (16–18), which may be mechanistically related to a loss of mitochondrial Δψ in certain contexts (19, 20). Necrosis had long been viewed as an unregulated consequence of catastrophic cell injury, but it is now clear that certain instances of necrosis can be programmed and thus considered modes of PCD. During necrotic PCD, mitochondrial swelling and loss of Δψ are thought to cause the evacuation of prodeath factors, which contribute to the demise of the cell (19). Indeed, the developmental stage during which we observed mitochondrial swelling and a loss of Δψ corresponded with the stage during which the DNA of discarded meiotic products are fragmented by the mitochondrial endonuclease G family member Nuc1 during PND (6). These findings prompted us to consider if organelle swelling might be a general feature of meiotic mother cells.

Although programmed cell death mechanisms are remarkably diverse, organelle swelling may be a unifying hallmark of necrotic forms of PCD (18, 21). The large size and well-understood fission and fusion dynamics of the yeast vacuole make this organelle a good candidate for further investigation of organelle swelling following meiosis. Moreover, the mother cell vacuole also undergoes programmed rupture at later stages of sporulation, highlighting its potential importance to PCD-related processes operating during sporulation (6). Using a strain expressing a Vma1-green fluorescent protein (GFP) fusion that marks the vacuolar membrane together with H2A-mCherry to monitor meiotic progression, we found that cells that had completed meiosis but had not yet executed vacuolar lysis possessed fewer, but larger, vacuoles than did meiotic cells (Fig. 2A). To determine if this apparent vacuolar coalescence was developmentally programmed, we engineered these markers into a strain that enables the conditional expression of *NDT80*, which encodes a transcription factor required for pro-

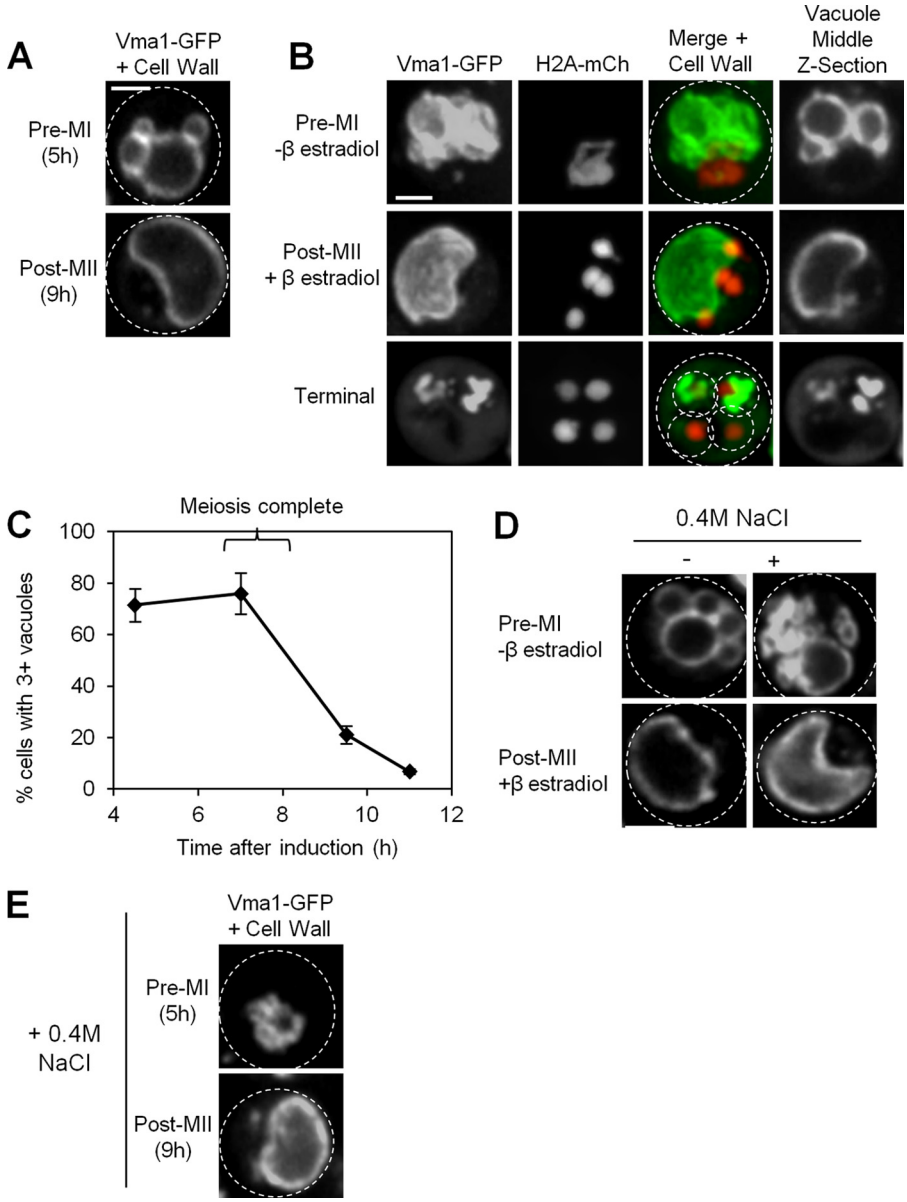

FIG 2 Meiotic mother cells undergo vacuole fusion and lysis. (A) Vacuoles of WT cells before (top) and after (bottom) meiosis. (B and C) Examination of vacuole size, number, and stability changes during sporulation utilizing induced expression of *NDT80* through β-estradiol addition at 5.5 h postinduction. Data points represent means ± standard deviations ($N = 3$; $n > 150$). (D) Response of pachytene-arrested cells and postmeiotic cells to treatment with 0.4 M NaCl for 10 min. The stress response was assessed 9 h after sporulation induction or 3.5 h following the addition of β-estradiol or the control treatment. (E) Stress responses of vacuoles of WT cells before (top) and after (bottom) meiosis. Vacuoles were visualized with Vma1-GFP, with the cell wall being indicated with a dotted line. Bars = 2 μm (all panels).

gression beyond the pachytene stage of meiosis (22, 23). In this system, *NDT80* expression is placed under the control of a promoter whose induction is dependent on the addition of β-estradiol to the culture medium (24, 25). As expected, we found that cells that sporulated in the absence of β-estradiol arrested at pachytene with a characteristic single large nucleus (Fig. 2B). Evaluation of Vma1-GFP revealed that these meiotically arrested cells possessed numerous distinct vacuoles (Fig. 2B). Following the addition of β-estradiol, these cells proceeded through meiosis and shortly thereafter dramatically coalesced their vacuoles into a significantly reduced number (often 1) of large and bloated organelles (Fig. 2B and C). Consistent with our previously reported findings (6), progression to terminal sporulation was associated with the dissolution of the mother cell vacuole. Of note, all of our Vma1-GFP experiments employed strains that are heterozygous for this transgene, and accordingly, we detected apparent spore-autonomous vacuolar biogenesis, as evaluated by the accumulation Vma1-GFP in 2 of the 4 spores (Fig. 2B). As uninduced cells maintained a multivacuolated phenotype until the induction of meiotic divisions via *NDT80* and the accompanying commitment to sporulation, we conclude that vacuolar coalescence is an additional feature of cells that are committed to sporulation.

Like many organelles, the yeast vacuole undergoes regulated fusion and fission to control vacuole number and size (26, 27). We hypothesized that modulation of fusion/fission dynamics might contribute to vacuole swelling in postmeiotic cells. We therefore examined the response of postmeiotic vacuoles to environmental cues that alter fission/fusion dynamics. Exposure of yeast cells to hypertonic stress is well documented to induce vacuole fission (26). Using the conditional *NDT80* expression strains as described above, we treated both premeiotic pachytene-arrested cells (which maintained numerous vacuoles) and postmeiotic cells (which typically possessed a single, enlarged vacuole) with 0.4 M NaCl to induce vacuole fission. Cells were allowed to sporulate, induced to express *NDT80*, or received control treatment and subsequently exposed to hypertonic stress for 10 min immediately prior to imaging. Postmeiotic cells were examined immediately after meiotic nuclear divisions, prior to visible spore wall deposition. Premeiotic cells divided their vacuoles into many smaller vesicles upon exposure to NaCl (Fig. 2D). In contrast to this, postmeiotic cells did not induce vacuolar fission when treated with 0.4 M NaCl, although they appeared to alter their shape (Fig. 2D). Identical vacuolar NaCl response characteristics were observed for cells with no *NDT80* manipulation, ruling out the possibility that estradiol treatment somehow contributed to this phenomenon (Fig. 2E).

Numerous studies have suggested that *NDT80* controls the commitment to meiosis and spore formation (28). Our findings identify a transition in mother cell vacuolar dynamics as an additional downstream consequence of *NDT80*-mediated commitment to gametogenesis. This commitment was characterized by a loss of the vacuole's capacity to undergo fission, its subsequent coalescence and swelling, and culminated in its lysis (6).

Vacuolar lysis and altered plasma membrane functionality coincide. Our findings suggest that meiotic mother cells execute PCD that exhibits features often associated with necrosis. Necrosis culminates in the loss of plasma membrane integrity, although other forms of PCD can also display this as part of a phenomenon known as "secondary necrosis" (29). To evaluate plasma membrane function during sporulation, we stained live cells at various stages of sporulation with propidium iodide (PI), a nucleic acid-binding dye commonly used to distinguish inviable cells that have died through either PCD or unregulated means. Necrotic and "secondary necrotic" cells stain positively with PI, reflecting a loss of plasma membrane-mediated PI exclusion. We utilized a low-carbon sporulation protocol for these experiments to induce reductions in spore number, thus ensuring that some nuclei would remain within the mother cell and serve as a substrate for potential PI staining. In contrast to meiotic cells, cells that had completed spore formation exhibited a pronounced accumulation of PI in the mother cell that was restricted from the spores (Fig. 3A). By examining cells throughout sporulation time courses for PI staining, we determined that only mother cells containing mature spores stained positively for PI, becoming PI positive ~6 to 7 h following the completion of meiosis (Fig. 3A and B). This indicated that perturbation of mother cell plasma membrane function was a late-acting occurrence during sporulation.

The acquisition of PI staining in meiotic mother cells coincided with the developmental stages at which we previously observed the lysis of the vacuole (6). This suggested that vacuolar lysis might contribute to the loss of plasma membrane function in meiotic mother cells. We therefore evaluated PI staining in postmeiotic cells together with the Vma1-GFP marker. Indeed, we found that only cells that had lost vacuolar membrane integrity stained positively with PI (Fig. 3C).

To further investigate this phenomenon, we examined the properties of the plasma membrane during sporulation by fusing mCherry-encoding sequences to *PMA1*, which encodes an abundant plasma membrane proton pump. As expected, Pma1-mCherry localized to the cell periphery under conditions of standard yeast growth in rich medium with glucose. Curiously, in the strain background that we utilized for these studies, SK1, we found that the mCherry signal was also detectable in the vacuolar lumen (Fig. 3D). As a similar phenomenon was previously reported to be a consequence of compromised accumulation of long-chain fatty acids in a different yeast strain background (30), we speculate that this unexpected dual localization may be attributable to strain background-specific alterations in the lipid composition of the plasma membrane. Nevertheless, Pma1-mCherry localization to the cell periphery predominated in meiotic mother cells. As cells progressed into postmeiotic stages, we observed that the Pma1-mCherry signal surrounding the mother cell disintegrated in cells that had lost Vma1-GFP continuity (Fig. 3D). Consistent with our observations of PI staining, we found that mother cells began to lose the Pma1-mCherry signal at the cell periphery ~6 h after the completion of meiosis (Fig. 3E). Thus, the lysis of the vacuole and loss of the continuous peripheral Pma1-mCherry signal appeared to be strictly coregulated: we were never able to identify cells that had lost the peripheral Pma1-mCherry signal yet maintained an intact, continuous vacuolar membrane ($n = 3$; $n > 200$). As we reported previously, meiotic synchrony and efficiency are mildly reduced in low-carbon compared with high-carbon sporulations (compare Fig. 3B and E) (6).

We previously found that inhibition of vacuolar proteolysis using the serine protease inhibitor phenylmethylsulfonyl fluoride (PMSF) caused a persistence of nuclear protein in mother cells executing PND, suggesting that vacuolar proteases directly contributed to their demise (6). In contrast to this, we found that PMSF treatment had no consequence on the acquisition of PI staining in the mother cell or the loss of the peripheral Pma1-mCherry signal (data not shown). While we cannot rule out the possibility that the loss of vacuolar membrane integrity and these symptoms of plasma membrane dysfunction are merely coincidental, we suspect that the release of vacuolar lipases that are not inhibited by PMSF may have a crucial role in this process.

Spore morphogenesis mutants execute abnormal cell death. We conclude that yeast meiotic mother cells undergo PCD that culminates in their autolysis. Reasoning that a critical level of spore morphogenesis is required to protect mother cells from the destructive milieu in which they develop, we hypothesized that meiotic mother cell PCD is developmentally coordinated with spore morphogenesis. This hypothesis predicts that PCD and spore morphogenesis share common elements of control and that perturbation of spore morphogenesis would therefore alter the fate of the dying mother cell. To gain insight into the control of mother cell PCD, we therefore examined the execution of PCD in mutants defective in specific steps of spore development. We focused our analysis on 10 gene mutations that permit normal meiosis but cause defects in specific stages of spore morphogenesis. Inclusive to this analysis are genes that promote prospore membrane closure, deposition of the inner cell wall (mannan and

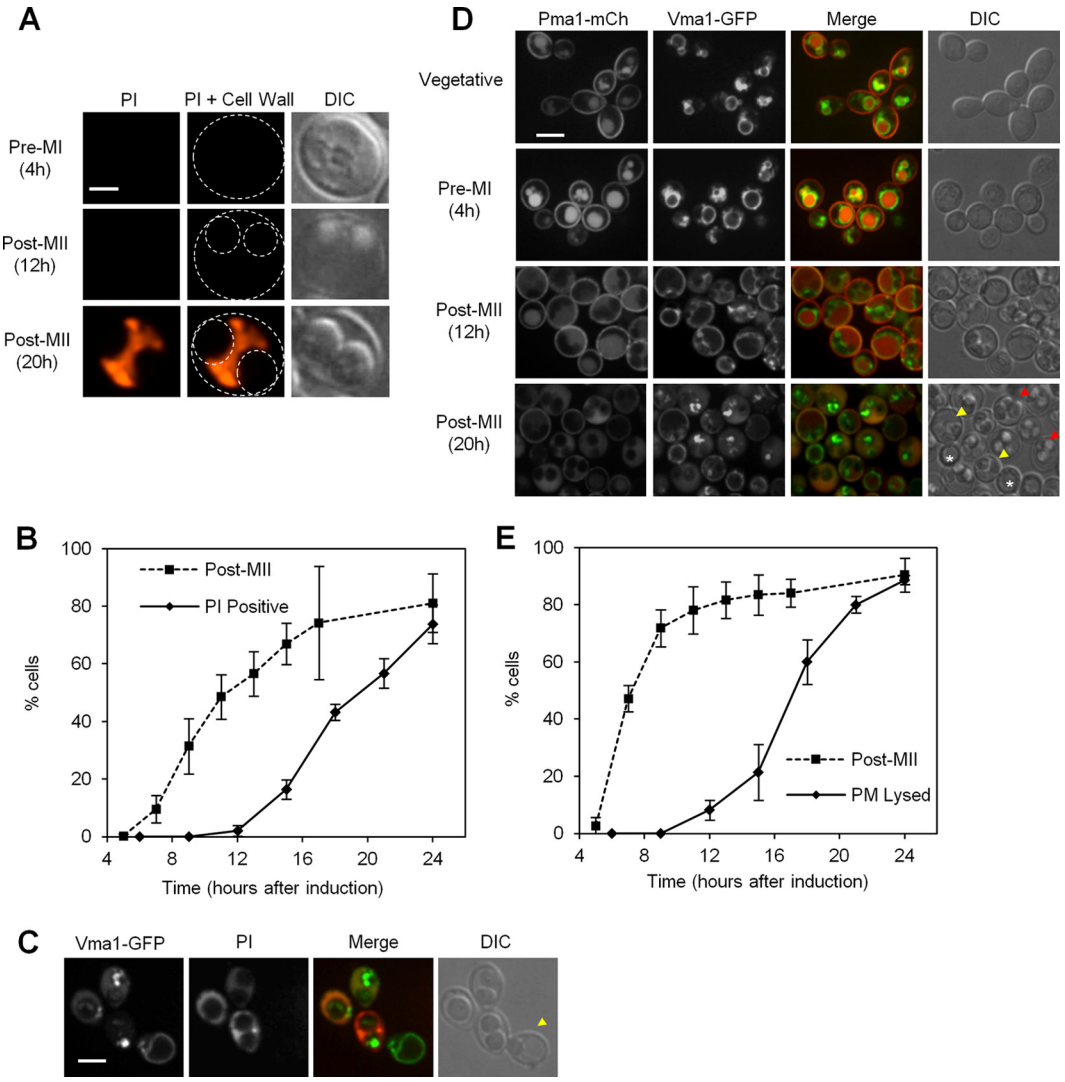

FIG 3 Meiotic mother cells lose plasma membrane integrity upon vacuole lysis. (A) Propidium iodide (PI) staining of cells at early (pre-MI) (4 h postinduction), post-MII (12 h postinduction), and late (20 h postinduction) stages of sporulation. (B) Quantification of the acquisition of PI staining relative to the completion of meiosis II (MII). (C) Cells expressing Vma1-GFP were stained with PI at 20 h postinduction. An example of a PI-negative cell with a continuous vacuolar membrane is indicated with a yellow triangle. (D) Pma1-mCherry and Vma1-GFP localization in mitotic cells in rich medium (top) and at 4 h (mid-meiotic), 12 h (postmeiotic), and 20 h postinduction (successive bottom panels). Examples of cells maintaining Vma1-GFP and Pma1-mCherry continuity are indicated in yellow, and examples where the membrane localization of both markers is lost are indicated in red. Asterisks indicate unsporulated cells; single focal planes are shown. (E) Quantification of the loss of Pma1-mCherry continuity relative to the completion of MII. All data points represent means ± standard deviations ($n = 3$; $n > 150$). Bars = 2 μm (A) and 5 μm (C and D).

β-glucan), and assembly of the outer spore coat (chitosan and dityrosine) (Fig. 4A and Table 1) (1, 31–38).

We allowed each of these mutants to sporulate to completion (24 h after induction) and assessed the condition of the mother cell vacuole using Vma1-GFP. We found that only 1 of the 10 mutants analyzed, *chs3*Δ, exhibited a complete loss of distinctive and contiguous GFP signals characteristic of lysed vacuoles in wild-type (WT) cells (Fig. 4B; see also Fig. S1 in the supplemental material). *CHS3* encodes a chitin synthase required for chitosan production. Notably, *chs3*Δ mutants progressed further into spore morphogenesis than did most of the other mutants examined, depositing the mannan and β-glucan layers but lacking the chitosan and dityrosine layers (1, 35). In stark contrast to the *chs3*Δ mutant, each of the other 9 mutants exhibited a 100% penetrant distinctive collapse of the vacuole into a disorganized mass with an intense GFP signal ($n > 200$ for each mutant) (Fig. 4B and Table 1; see also Fig. S1 in the supplemental material). This vacuolar collapse was not observed in *ndt80*Δ cells, which arrest prior to meiosis I and maintain intact vacuoles, suggesting that this is a characteristic of cells that commit to meiotic completion but do not achieve prospore formation and/or early spore wall synthesis (see Fig. S1 in the supplemental material).

The abnormal terminal vacuolar morphology of spore morphogenesis mutants suggested that the mother cells were dying through alternative mechanisms. Indeed, perturbation of PCD execution in animals is often associated with the death of the cells through alternative means (39). To explore this further, we systematically assessed the survival of the abnormally developed

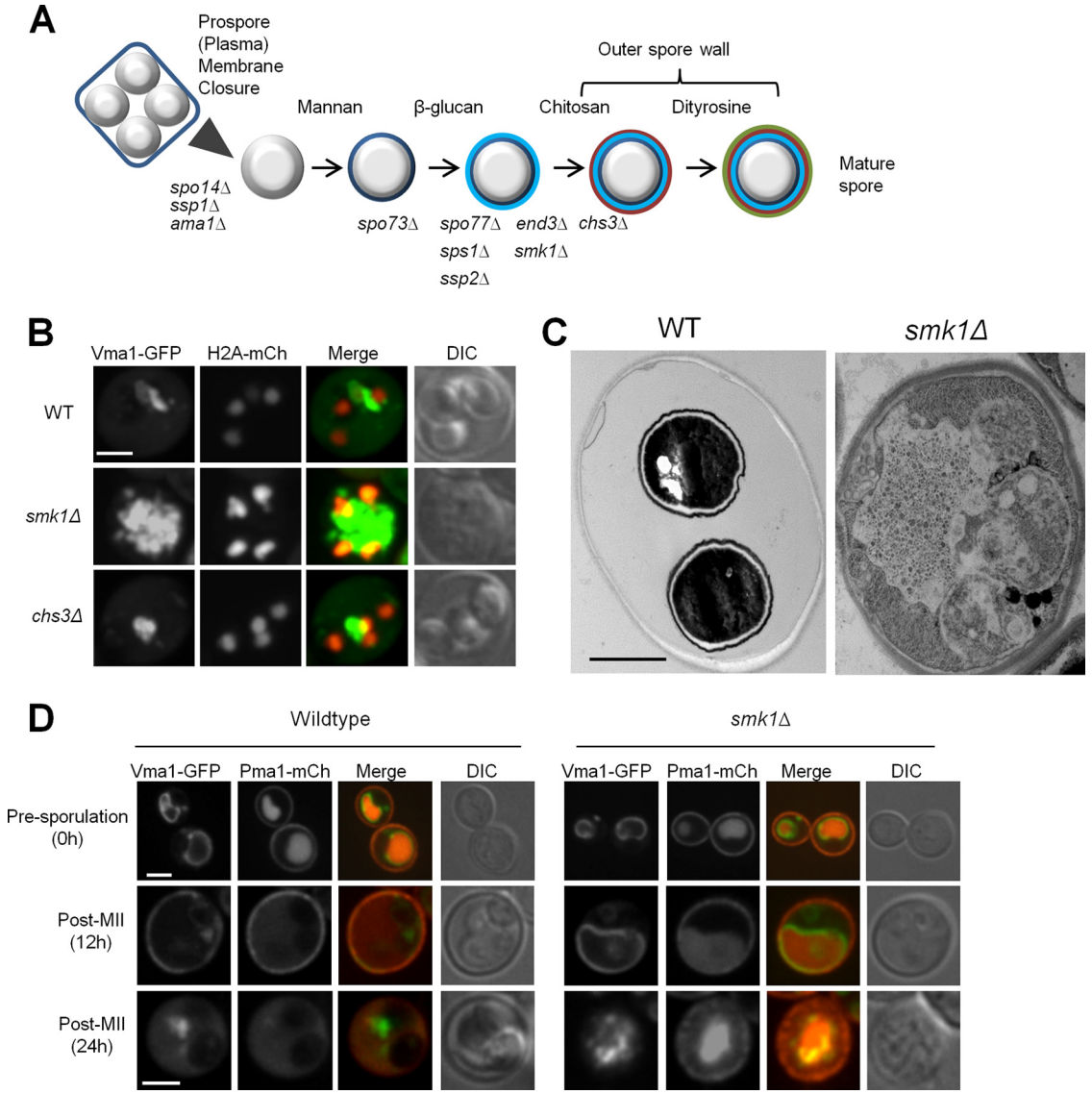

FIG 4 PCD of the meiotic mother cell is distinct in spore morphogenesis mutants. (A) Each of the sporulation mutants that we examined disrupt specific morphogenic events ranging from prospore closure to outer spore wall synthesis. Mutant genotypes are aligned below the stage at which they are arrested. (B) Terminal vacuole morphology phenotypes in sporulated WT, *smk1*Δ, and *chs3*Δ cells. (C) TEM of WT and *smk1*Δ cells 24 h after sporulation induction. (D) Plasma membrane and vacuole integrity in WT and *smk1*Δ cells at presporulation (0 h), post-MII (12 h), and terminal (24 h) time points. Single middle z-sections are shown. Bars = 2 μm in all images.

spores produced by these mutants by quantifying the fraction of meiotic mother cells capable of forming a colony. This analysis revealed that, with the exception of the *chs3*Δ mutant, all of the mutants caused a dramatic loss of spore viability (Table 1), demonstrating that they indeed lose viability and that dysregulated meiotic mother cell PCD is correlated with the death of the immature spores. Of course, the reduced robustness of these poorly developed spores likely sensitized them to the consequences of the death of their host cell, underscoring the importance of developmental coordination of spore differentiation and PCD.

Among the mutants that perturbed mother cell PCD was a mutant with a deletion of *SMK1*, which encodes a sporulation-dedicated mitogen-activated protein (MAP) kinase with complex contributions to spore wall formation (40). Owing to *SMK1*'s relatively late function in the spore morphogenesis pathway (Fig. 4A) and significant degree of characterization (1, 32, 36, 40), we further interrogated *smk1*Δ cells to explore the characteristics of this alternative cell death (Fig. 4B). Transmission electron micrographs revealed that terminally sporulated *smk1*Δ mutants did not exhibit clearance of the mother cell cytoplasm, as is characteristic of terminally sporulated WT cells, and instead possessed electron-dense, collapsed vacuoles that appeared partially contiguous with the immature spores (Fig. 4C). Live-cell fluorescence imaging revealed that the plasma and vacuolar membranes of *smk1*Δ cells appeared similar to those of WT cells at early and middle stages of sporulation. However, in contrast to what occurs in WT cells, a substantial amount of Pma1-mCherry signal appeared to remain at the cell periphery in terminally sporulated *smk1*Δ cells

TABLE 1 Vacuole and gamete viability phenotypes of spore morphogenesis mutants

Strain	Spore morphogenesis defect(s) (reference[s])	Vacuole phenotype upon death[a]	% of viable cells following meiosis
*spo14*Δ	Prospore membrane assembly (33)	Collapsed	18
*ssp1*Δ	Prospore membrane closure (34)	Collapsed	18
*ama1*Δ	Prospore membrane closure (38)	Collapsed	10.5
*spo73*Δ	β-Glucan, outer spore wall synthesis (35)	Collapsed	2.5
*spo77*Δ	Outer spore wall synthesis (35)	Collapsed	7.6
*sps1*Δ	Pleiotropic; outer spore wall synthesis (31)	Collapsed	29
*ssp2*Δ	Outer spore wall synthesis (35)	Collapsed	20
*smk1*Δ	Pleiotropic; outer spore wall synthesis (32, 36)	Collapsed	16
*end3*Δ	Outer spore wall synthesis (37)	Collapsed	0.7
*chs3*Δ	Outer spore wall synthesis (35)	Lysed	74.7
WT	NA	Lysed	99.9

[a] Vacuoles were judged to be either "collapsed" or "lysed" by Vma1-GFP, as described in the text. The percentage of viable cells was determined by CFU per volume, as described in Materials and Methods. NA, not applicable.

(Fig. 4D). We therefore conclude that mother cell death in *smk1*Δ mutants is morphologically distinct from WT PCD and is not accompanied by normal vacuole lysis, cytoplasmic clearance, or loss of the plasma membrane proton pump.

To gain more insight into the role of *SMK1* in PCD, we examined the vacuole during sporulation time courses and found that its intactness persisted in *smk1*Δ mutants at points in late sporulation when WT cells had executed vacuolar lysis (Fig. 5A). As mentioned above, following this period of defective vacuolar lysis, the vacuoles of *smk1*Δ cells collapsed into a disorganized mass (Fig. 4B). Confirming previously reported findings, *smk1*Δ cells underwent meiosis with kinetics essentially identical to those of the WT (32), indicating that their delay in vacuolar lysis was not due to slower meiotic progression and that *SMK1*-dependent events are required to coordinate the transition from meiotic completion to mother cell death (Fig. 5B). We observed that refractile spore wall deposition was discernible in *smk1*Δ cells prior to the collapse of the mother cell vacuole, consistent with previously reported observations showing that *smk1*Δ cells are capable of inner spore wall deposition but are defective in forming the outer spore wall (32) (Fig. 5A). However, we never observed similarly discernible spore walls in *smk1*Δ cells that had sporulated terminally and undergone vacuolar collapse (Fig. 4B and D), suggesting that the integrity of underdeveloped *smk1*Δ spores became compromised upon mother cell death. Indeed, a previous study found that the viability of spores produced by *smk1*Δ mutants declined as these cells persisted in sporulation medium (32). Our findings show that in addition to its defects in directing spore morphogenesis, *smk1*Δ also causes defects in the morphology and developmental timing of mother cell PCD. Interpretation of the *smk1*Δ phenotype thus offers the most straightforward support for the conclusion that PCD and spore morphogenesis are developmentally coordinated through common genetic mechanisms.

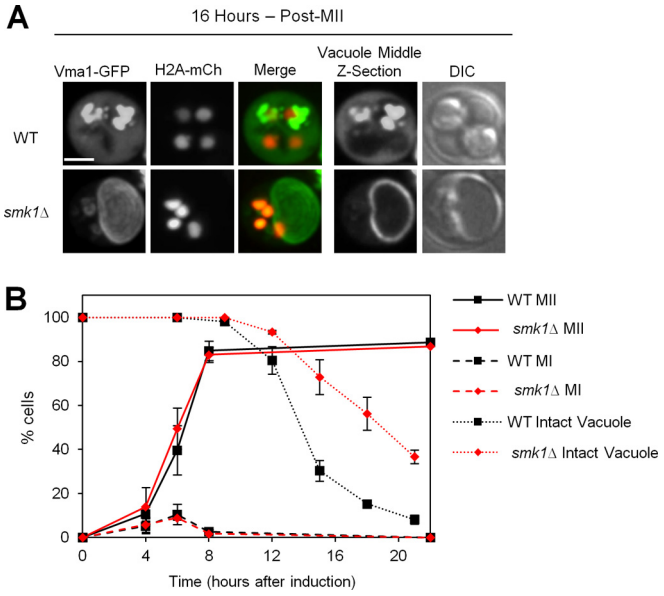

FIG 5 *smk1*Δ cells abnormally maintain vacuoles following meiosis. (A) WT and *smk1*Δ cells 16 h after sporulation induction. (B) Quantification of vacuole integrity relative to the completion of MI and MII in WT and *smk1*Δ strains. Data points represent means ± standard deviations ($n = 3$; $n > 150$). Vacuoles were scored as either continuous or discontinuous, with no distinction for morphology following the loss of integrity. Bar = 2 μm.

DISCUSSION

Our findings identify sporulation as a bona fide context of PCD in yeast. Symptoms of mother cell death become apparent very early, manifested by a loss of both mitochondrial Δψ and the capacity for vacuolar fusion very soon after the spore contents become segregated from the mother cell. Following this, we observed vacuolar rupture and the loss of plasma membrane integrity occurring in a coordinate manner. We furthermore showed that mutations that perturbed prospore construction and/or inner spore wall formation displayed altered cell death with morphology and developmental timing distinct from those of WT cells. This indicates that gamete development and mother cell PCD are coordinated by common genetic pathways, although the precise mechanisms by which this coordination occurs remain to be determined.

The swelling and permeabilization of the vacuole and mitochondria, along with the accompanying loss of mitochondrial Δψ, invite comparisons of meiotic mother cell death with programmed necrosis observed in animals. Mother cell death is programmed in the classical sense in that it occurs invariably during development and in that its execution requires specific gene products. It also displays unique hallmarks among known modes of yeast PCD: we are unaware of any context in which the vacuole undergoes such dramatic alterations in size, number, and permeability during

PCD. Additionally, we have been unable to identify numerous phenomena that have been described to occur during the demise of vegetative yeast cells during meiotic mother cell death. For example, stress-induced PCD of vegetative yeast elicits phosphatidylserine exposure on the outer plasma membrane, which is detected by annexin V staining (7). At no point in sporulation were we able to detect annexin V-positive cells (data not shown), indicating that meiotic mother cell death is distinct from stress-induced PCD of vegetative yeast in this respect. With the exception of *NUC1* (6), we also have yet to uncover detectable roles for yeast orthologs of animal apoptotic regulators such as Yca1 and Aif1 (41) in the phenomena presented in this study, although further exploration of their contributions to sporulation may yet be informative.

How might meiotic PCD relate to the phenomenon of PCD in vegetative yeast cells (41)? We point out that, like most yeast studies, studies of yeast PCD in vegetative cells have been carried out exclusively with highly domesticated strains artificially locked in the haploid phase of the yeast life cycle and thus precluded from any possibility of engaging meiotic PCD. Moreover, the context that has been most often suggested to represent the altruistic and adaptive application of haploid cell death, starvation, also represents conditions under which diploid cells execute meiosis. We thus speculate that at least some of the characteristics of haploid yeast PCD under such conditions represent a vestigial application of the meiotic PCD program.

Probing the role of vacuolar hydrolases in mother cell PCD has proven challenging because all stages of sporulation are acutely sensitive to inhibition of vacuolar nutrient turnover and most mutants that perturb vacuolar function fail to sporulate. Although the serine protease inhibitor PMSF inhibits nuclear protein turnover during PND (6), we found that PMSF treatment did not detectably alter any of the other phenomena occurring during mother cell death that we describe here (data not shown). We anticipate that further elucidation of the mechanisms underlying meiotic mother cell PCD will be relevant for understanding the modes of programmed necrosis or other forms of PCD that exhibit vacuole/lysosome permeabilization and, more generally, for understanding the interconnectedness and regulation of organelle dynamics during PCD.

The primary questions arising from this study concern the mechanism through which spore morphogenesis and mother cell death are coordinated. We showed that numerous mutations that perturb early spore morphogenesis also result in abnormal mother cell death, implying that spore development is required for normal mother cell PCD to occur. We speculate that the alternative terminal characteristics that we observed in these mutants may reflect death caused by the catastrophic inability of the mother cell to sustain viability in the absence of proper PCD signaling. The delayed occurrence of vacuole rupture during this mode of death in *smk1*Δ mutants is consistent with the existence of a checkpoint that ensures a critical level of spore development prior to mother cell PCD execution. When a cell commits to sporulation but is incapable of reaching this threshold level of gamete development and therefore incapable of initiating PCD, it may be confined to an unsustainable arrest stage that eventually leads to the death of the mother cell and its underdeveloped spores.

Our analysis indicates that the construction of the outer spore layers of chitosan and dityrosine are dispensable for mother cell death *per se*, as *chs3*Δ cells lacking the outer spore coat execute PCD apparently normally. Spores lacking *CHS3* also do not exhibit a substantial loss of viability upon germination, demonstrating that the inner spore wall layers are largely sufficient to protect spores from the destructive processes that occur around them. We therefore speculate that the initiation of PCD may accompany the developmental events that cue the transition to from β-glucan to chitosan synthesis. Consistent with this, the MAP kinase Smk1 promotes this transition through its interaction with the β-glucan synthase Gsc2 (36), and we find that *SMK1* is essential for proper PCD execution. However, *smk1*Δ cells display some heterogeneity with regard to the degree of development achieved within an individual ascus (32), and the abnormal PCD may thus reflect additional defects. Of course, an additional interpretation of our findings is that Smk1 may also participate directly in promoting PCD. Intriguingly, the MAP kinase gene *mpk-1* positively regulates apoptosis-like death of immature germ cells in the syncytial *Caenorhabditis elegans* gonad in a phenomenon that is conceptually similar to yeast meiotic mother cell death (42, 43). Further exploration of the control mechanisms by which Smk1 impacts meiotic PCD will illuminate these possibilities.

Our findings highlight morphogenesis as a general context to consider PCD in microbes. In a manner analogous to the role of PCD in the removal of unneeded cells during metazoan development, yeast meiotic mother cell death eliminates a superfluous cell remnant during a developmental transition. Remarkably, a similar host cell death phenomenon accompanies endospore formation in the bacterium *Bacillus subtilis*. In response to starvation, *B. subtilis* undergoes asymmetric division, after which the smaller presumptive spore is engulfed by its larger sibling cell to form a sporangium. The sporangium then hosts endospore formation and undergoes autolysis coordinate with spore development (44, 45). Thus, similarly to what we describe for yeast sporulation, *B. subtilis* sporulation coordinates the morphogenesis of a daughter cell with the programmed death of its progenitor. Although there is no evidence to suggest that microbial cell death pathways in prokaryotes and eukaryotes share a common genetic regulation, the provocatively similar cell biological events underlying PCD in *B. subtilis* and that in *S. cerevisiae* invite evolutionary questions: does PCD represent a convergent target of evolution and thus have numerous genetic origins? Certainly, the ever-growing diversity in discovered forms of PCD and their according genetic control mechanisms seems consistent with this idea.

ACKNOWLEDGMENTS

We thank Brenda Andrews, Charlie Boone, Angelika Amon, and Lars Steinmetz for sharing yeast strains; Kiersten Henderson for advice concerning the construction of Pma1-mCherry strains; and Jason Moffat for the sharing imaging equipment. Doug Holmyard and the Advanced Bioimaging Centre at Mt. Sinai Hospital, Toronto, provided technical assistance with electron microscopy.

This work was supported by an NSERC discovery grant and CIHR grant MOP-89996 to M.D.M.

REFERENCES

1. **Neiman AM.** 2011. Sporulation in the budding yeast Saccharomyces cerevisiae. Genetics **189:**737–765. http://dx.doi.org/10.1534/genetics.111.127126.
2. **Brewer BJ, Fangman WL.** 1980. Preferential inclusion of extrachromosomal genetic elements in yeast meiotic spores. Proc Natl Acad Sci U S A **77:**5380–5384. http://dx.doi.org/10.1073/pnas.77.9.5380.
3. **Davidow LS, Goetsch L, Byers B.** 1980. Preferential occurrence of nonsister spores in two-spored asci of Saccharomyces cerevisiae: evidence for

regulation of spore-wall formation by the spindle pole body. Genetics **94:**581–595.
4. **Taxis C, Keller P, Kavagiou Z, Jensen LJ, Colombelli J, Bork P, Stelzer EH, Knop M.** 2005. Spore number control and breeding in Saccharomyces cerevisiae: a key role for a self-organizing system. J Cell Biol **171:**627–640. http://dx.doi.org/10.1083/jcb.200507168.
5. **Nickas ME, Diamond AE, Yang MJ, Neiman AM.** 2004. Regulation of spindle pole function by an intermediary metabolite. Mol Biol Cell **15:**2606–2616. http://dx.doi.org/10.1091/mbc.E04-02-0128.
6. **Eastwood MD, Cheung SW, Lee KY, Moffat J, Meneghini MD.** 2012. Developmentally programmed nuclear destruction during yeast gametogenesis. Dev Cell **23:**35–44. http://dx.doi.org/10.1016/j.devcel.2012.05.005.
7. **Buttner S, Eisenberg T, Carmona-Gutierrez D, Ruli D, Knauer H, Ruckenstuhl C, Sigrist C, Wissing S, Kollroser M, Frohlich KU, Sigrist S, Madeo F.** 2007. Endonuclease G regulates budding yeast life and death. Mol Cell **25:**233–246. http://dx.doi.org/10.1016/j.molcel.2006.12.021.
8. **Aram L, Arama E.** 2012. Sporoptosis: sowing the seeds of nuclear destruction. Dev Cell **23:**5–6. http://dx.doi.org/10.1016/j.devcel.2012.06.016.
9. **Turk B, Turk V.** 2009. Lysosomes as "suicide bags" in cell death: myth or reality? J Biol Chem **284:**21783–21787. http://dx.doi.org/10.1074/jbc.R109.023820.
10. **Boya P, Kroemer G.** 2008. Lysosomal membrane permeabilization in cell death. Oncogene **27:**6434–6451. http://dx.doi.org/10.1038/onc.2008.310.
11. **Buser C, Drubin DG.** 2013. Ultrastructural imaging of endocytic sites in Saccharomyces cerevisiae by transmission electron microscopy and immunolabeling. Microsc Microanal **19:**381–392. http://dx.doi.org/10.1017/S1431927612014304.
12. **Zamzami N, Marchetti P, Castedo M, Zanin C, Vayssiere JL, Petit PX, Kroemer G.** 1995. Reduction in mitochondrial potential constitutes an early irreversible step of programmed lymphocyte death in vivo. J Exp Med **181:**1661–1672. http://dx.doi.org/10.1084/jem.181.5.1661.
13. **Kroemer G, Galluzzi L, Brenner C.** 2007. Mitochondrial membrane permeabilization in cell death. Physiol Rev **87:**99–163. http://dx.doi.org/10.1152/physrev.00013.2006.
14. **Green DR, Kroemer G.** 2004. The pathophysiology of mitochondrial cell death. Science **305:**626–629. http://dx.doi.org/10.1126/science.1099320.
15. **Hughes AL, Gottschling DE.** 2012. An early age increase in vacuolar pH limits mitochondrial function and lifespan in yeast. Nature **492:**261–265. http://dx.doi.org/10.1038/nature11654.
16. **Zong WX, Thompson CB.** 2006. Necrotic death as a cell fate. Genes Dev **20:**1–15. http://dx.doi.org/10.1101/gad.1376506.
17. **Linkermann A, Green DR.** 2014. Necroptosis. N Engl J Med **370:**455–465. http://dx.doi.org/10.1056/NEJMra1310050.
18. **Chan FK.** 2012. Fueling the flames: mammalian programmed necrosis in inflammatory diseases. Cold Spring Harb Perspect Biol **4:**a008805. http://dx.doi.org/10.1101/cshperspect.a008805.
19. **Kitsis RN, Molkentin JD.** 2010. Apoptotic cell death "nixed" by an ER-mitochondrial necrotic pathway. Proc Natl Acad Sci U S A **107:**9031–9032. http://dx.doi.org/10.1073/pnas.1003827107.
20. **Vaseva AV, Marchenko ND, Ji K, Tsirka SE, Holzmann S, Moll UM.** 2012. p53 opens the mitochondrial permeability transition pore to trigger necrosis. Cell **149:**1536–1548. http://dx.doi.org/10.1016/j.cell.2012.05.014.
21. **Vanden Berghe T, Linkermann A, Jouan-Lanhouet S, Walczak H, Vandenabeele P.** 2014. Regulated necrosis: the expanding network of non-apoptotic cell death pathways. Nat Rev Mol Cell Biol **15:**135–147. http://dx.doi.org/10.1038/nrm3737.
22. **Xu L, Ajimura M, Padmore R, Klein C, Kleckner N.** 1995. NDT80, a meiosis-specific gene required for exit from pachytene in Saccharomyces cerevisiae. Mol Cell Biol **15:**6572–6581.
23. **Pak J, Segall J.** 2002. Role of Ndt80, Sum1, and Swe1 as targets of the meiotic recombination checkpoint that control exit from pachytene and spore formation in Saccharomyces cerevisiae. Mol Cell Biol **22:**6430–6440. http://dx.doi.org/10.1128/MCB.22.18.6430-6440.2002.
24. **Benjamin KR, Zhang C, Shokat KM, Herskowitz I.** 2003. Control of landmark events in meiosis by the CDK Cdc28 and the meiosis-specific kinase Ime2. Genes Dev **17:**1524–1539. http://dx.doi.org/10.1101/gad.1101503.
25. **Carlile TM, Amon A.** 2008. Meiosis I is established through division-specific translational control of a cyclin. Cell **133:**280–291. http://dx.doi.org/10.1016/j.cell.2008.02.032.
26. **Weisman LS.** 2003. Yeast vacuole inheritance and dynamics. Annu Rev Genet **37:**435–460. http://dx.doi.org/10.1146/annurev.genet.37.050203.103207.
27. **Michaillat L, Mayer A.** 2013. Identification of genes affecting vacuole membrane fragmentation in Saccharomyces cerevisiae. PLoS One **8:**e54160. http://dx.doi.org/10.1371/journal.pone.0054160.
28. **Winter E.** 2012. The Sum1/Ndt80 transcriptional switch and commitment to meiosis in Saccharomyces cerevisiae. Microbiol Mol Biol Rev **76:**1–15. http://dx.doi.org/10.1128/MMBR.05010-11.
29. **Majno G, Joris I.** 1995. Apoptosis, oncosis, and necrosis. An overview of cell death. Am J Pathol **146:**3–15.
30. **Toulmay A, Schneiter R.** 2007. Lipid-dependent surface transport of the proton pumping ATPase: a model to study plasma membrane biogenesis in yeast. Biochimie **89:**249–254. http://dx.doi.org/10.1016/j.biochi.2006.07.020.
31. **Friesen H, Lunz R, Doyle S, Segall J.** 1994. Mutation of the SPS1-encoded protein kinase of Saccharomyces cerevisiae leads to defects in transcription and morphology during spore formation. Genes Dev **8:**2162–2175. http://dx.doi.org/10.1101/gad.8.18.2162.
32. **Krisak L, Strich R, Winters RS, Hall JP, Mallory MJ, Kreitzer D, Tuan RS, Winter E.** 1994. SMK1, a developmentally regulated MAP kinase, is required for spore wall assembly in Saccharomyces cerevisiae. Genes Dev **8:**2151–2161. http://dx.doi.org/10.1101/gad.8.18.2151.
33. **Rudge SA, Cavenagh MM, Kamath R, Sciorra VA, Morris AJ, Kahn RA, Engebrecht J.** 1998. ADP-ribosylation factors do not activate yeast phospholipase Ds but are required for sporulation. Mol Biol Cell **9:**2025–2036. http://dx.doi.org/10.1091/mbc.9.8.2025.
34. **Moreno-Borchart AC, Strasser K, Finkbeiner MG, Shevchenko A, Shevchenko A, Knop M.** 2001. Prospore membrane formation linked to the leading edge protein (LEP) coat assembly. EMBO J **20:**6946–6957. http://dx.doi.org/10.1093/emboj/20.24.6946.
35. **Coluccio A, Bogengruber E, Conrad MN, Dresser ME, Briza P, Neiman AM.** 2004. Morphogenetic pathway of spore wall assembly in Saccharomyces cerevisiae. Eukaryot Cell **3:**1464–1475. http://dx.doi.org/10.1128/EC.3.6.1464-1475.2004.
36. **Huang LS, Doherty HK, Herskowitz I.** 2005. The Smk1p MAP kinase negatively regulates Gsc2p, a 1,3-beta-glucan synthase, during spore wall morphogenesis in Saccharomyces cerevisiae. Proc Natl Acad Sci U S A **102:**12431–12436. http://dx.doi.org/10.1073/pnas.0502324102.
37. **Morishita M, Engebrecht J.** 2005. End3p-mediated endocytosis is required for spore wall formation in Saccharomyces cerevisiae. Genetics **170:**1561–1574. http://dx.doi.org/10.1534/genetics.105.041459.
38. **Diamond AE, Park JS, Inoue I, Tachikawa H, Neiman AM.** 2009. The anaphase promoting complex targeting subunit Ama1 links meiotic exit to cytokinesis during sporulation in Saccharomyces cerevisiae. Mol Biol Cell **20:**134–145. http://dx.doi.org/10.1091/mbc.E08-06-0615.
39. **Vercammen D, Brouckaert G, Denecker G, Van de Craen M, Declercq W, Fiers W, Vandenabeele P.** 1998. Dual signaling of the Fas receptor: initiation of both apoptotic and necrotic cell death pathways. J Exp Med **188:**919–930. http://dx.doi.org/10.1084/jem.188.5.919.
40. **Wagner M, Briza P, Pierce M, Winter E.** 1999. Distinct steps in yeast spore morphogenesis require distinct SMK1 MAP kinase thresholds. Genetics **151:**1327–1340.
41. **Carmona-Gutierrez D, Eisenberg T, Buttner S, Meisinger C, Kroemer G, Madeo F.** 2010. Apoptosis in yeast: triggers, pathways, subroutines. Cell Death Differ **17:**763–773. http://dx.doi.org/10.1038/cdd.2009.219.
42. **Gumienny TL, Lambie E, Hartwieg E, Horvitz HR, Hengartner MO.** 1999. Genetic control of programmed cell death in the Caenorhabditis elegans hermaphrodite germline. Development **126:**1011–1022.
43. **Perrin AJ, Gunda M, Yu B, Yen K, Ito S, Forster S, Tissenbaum HA, Derry WB.** 2013. Noncanonical control of C. elegans germline apoptosis by the insulin/IGF-1 and Ras/MAPK signaling pathways. Cell Death Differ **20:**97–107. http://dx.doi.org/10.1038/cdd.2012.101.
44. **Allocati N, Masulli M, Di Ilio C, De Laurenzi V.** 2015. Die for the community: an overview of programmed cell death in bacteria. Cell Death Dis **6:**e1609. http://dx.doi.org/10.1038/cddis.2014.570.
45. **Hosoya S, Lu Z, Ozaki Y, Takeuchi M, Sato T.** 2007. Cytological analysis of the mother cell death process during sporulation in Bacillus subtilis. J Bacteriol **189:**2561–2565. http://dx.doi.org/10.1128/JB.01738-06.